

Ohmic Contacts to n-Type $\text{Al}_{0.6}\text{Ga}_{0.4}\text{N}$ for Solar-Blind Detectors

Zhu Yanling^{1,†}, Du Jiangfeng¹, Luo Muchang², Zhao Hong², Zhao Wenbo², Huang Lieyun²,
Ji Hong¹, Yu Qi¹, and Yang Mohua¹

(1 State Key Laboratory of Electronic Thin Films and Integrated Devices, University of Electronic Science and
Technology of China, Chengdu 610054, China)
(2 Chongqing Optoelectronics Research Institute, Chongqing 400060, China)

Abstract: We investigate the contact characteristics of bi-layer thin films, Ti (20nm)/Al (200nm) on Si-doped n-type $\text{Al}_{0.6}\text{Ga}_{0.4}\text{N}$ films grown on sapphire substrate. The surface treatment was aqua regia boiling before metallization and annealing after metallization at different conditions in N_2 ambient. High resolution X-ray diffractometry analysis was carried out on the contacts and the surface interfaces of these conditions were compared. A specific contact resistivity ρ_c was determined using the circular transmission line method via current-voltage measurements. A ρ_c of $3.42 \times 10^{-4} \Omega \cdot \text{cm}^2$ was achieved when annealed at 670°C for 90s. Then, this ideal ohmic contact was used in back-illuminated solar-blind AlGaIn p-i-n detectors and the detectors' performances, such as spectral responsivity, dark-current, and breakdown voltage were optimized.

Key words: high-Al content n-AlGaIn; ohmic contact; anneal; back-illumination; solar-blind p-i-n detector

PACC: 2940P; 6150C **EEACC:** 4250

CLC number: O47 **Document code:** A **Article ID:** 0253-4177(2008)09-1661-05

1 Introduction

At present, ultraviolet photodetectors have received much attention for their importance in solar-UV monitoring, space communications, missile detection, as well as flame and heat sensing applications. $\text{Al}_x\text{Ga}_{1-x}\text{N}$ is the optimum choice for fabricating these photodetectors owing to its wide bandgap. For the fabrication of photodetectors with a sharp transmission cut off wavelength at $\lambda < 280\text{nm}$, an Al mole fraction > 0.4 is required. Until now, not much research has been done on ohmic contacts to n-type $\text{Al}_x\text{Ga}_{1-x}\text{N}$ with $x > 0.3$. Adivarahan *et al.*^[1] reported that the specific contact resistivity of Ti/Al/Ti/Au ohmic contacts on n-type $\text{Al}_{0.4}\text{Ga}_{0.6}\text{N}$ was $2.5 \times 10^{-3} \Omega \cdot \text{cm}^2$.

The most widely used ohmic contact to n-type GaN is based on Al/Ti^[2,3]. The Ti-layer can significantly improve the contact resistance^[4]. The advantage of a Ti layer has been attributed to either the degenerate n^+ -surface layer resulting from the N-vacancy donor for the formation of the TiN compound or the Ti acting to reduce the surface oxide^[5]. In either case, the Al overlayer is superior to an Au overlayer, which suggests that Al/Ti alloy may play a role in the contact formation^[6]. Analogously, ohmic contacts to n-AlGaIn usually use the Ti/Al or Ti/Al/Ti/Au metalisation. Cao *et al.*^[2] reported the specific contact re-

sistivity of Ti/Al/Ti/Au ohmic contacts on n- $\text{Al}_{0.3}\text{Ga}_{0.7}\text{N}$ was $7 \times 10^{-5} \Omega \cdot \text{cm}^2$. Chen *et al.*^[7] reported the specific contact resistivity of Ti/Al/Ni/Au ohmic contacts on n- $\text{Al}_{0.45}\text{Ga}_{0.55}\text{N}$ was $2.75 \times 10^{-4} \Omega \cdot \text{cm}^2$.

In this paper, we report a low resistance ohmic metallization for an $\text{Al}_{0.6}\text{Ga}_{0.4}\text{N}$ layer by pre-metallization treatment in the surface using aqua regia and annealing after metallization. Additionally, we study the influence of the ohmic contacts on solar-blind detectors.

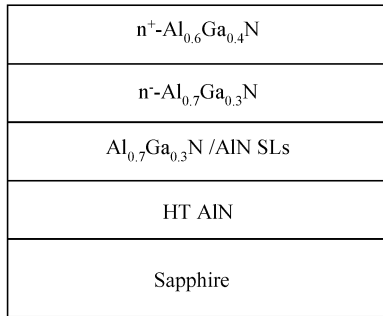
2 Experiments

The samples used in this study were grown on c-plane (0001) sapphire substrates by a low-pressure Aixtron 200 RF horizontal flow reactor metal organic chemical vapor deposition (MOCVD) system. Trimethylgallium (TMGa), Trimethylaluminum (TMAI), and ammonia (NH_3) were used as Ga, Al, and N precursors, respectively. Silane was used as the n-type dopant and H_2 was the carrier gas.

Figure 1 shows the schematic cross-section structure of the $\text{Al}_{0.6}\text{Ga}_{0.4}\text{N}$ sample. A 500nm-thick high-temperature AlN template layer was initially grown at 1180°C. Afterward, a 60nm-thick super lattice (SL) layer (5 periods $\text{Al}_{0.7}\text{Ga}_{0.3}\text{N}/\text{AlN}$) was grown at 1120°C to weaken the stress during the material growth. This layer was followed by a Si-doped n-AlGaIn layer grown at 1120°C. The Si-doped AlGaIn

† Corresponding author. Email: yanlz83@163.com

Received 26 March 2008, revised manuscript received 7 May 2008

Fig. 1 Schematic structure of $\text{Al}_{0.6}\text{Ga}_{0.4}\text{N}$ sample

consisted of two AlGa_xN layers with Al contents of 0.6 and 0.7, respectively. The thickness of the $\text{Al}_{0.7}\text{Ga}_{0.3}\text{N}$ layer and $\text{Al}_{0.6}\text{Ga}_{0.4}\text{N}$ layer are 400 and 750nm. The sample is a part of back-illuminated solar-blind $\text{Al}_x\text{Ga}_{1-x}\text{N}$ p-i-n photodiodes. So the $\text{Al}_{0.7}\text{Ga}_{0.3}\text{N}$ window layer was grown as the short wavelength cutoff region and $\text{Al}_{0.6}\text{Ga}_{0.4}\text{N}$ layer was used as the buffer layer. The Al mole fraction of 60% was established by Rutherford backscattering spectrometry (RBS). Room temperature Hall measurements exhibited the carrier concentration of $2.77 \times 10^{18} \text{cm}^{-3}$ and the mobility of $45.1 \text{cm}^2/(\text{V} \cdot \text{s})$.

In-situ optical reflectometry measurement was used to monitor the growth process. As shown in Fig. 2, the indicated region corresponds to: (1) the growth of HT-AlN; (2) the growth of the $\text{Al}_{0.7}\text{Ga}_{0.3}\text{N}/\text{AlN}$ super lattice layer; (3) the growth of the $\text{Al}_{0.7}\text{Ga}_{0.3}\text{N}$ layer; and (4) the growth of the $\text{Al}_{0.6}\text{Ga}_{0.4}\text{N}$ layer. That the peak values of the in-situ optical reflectance monitoring curves remain constant shows that the epitaxial layers are very smooth and have good quality.

The ohmic metallisation consisting of Ti (20nm)/Al (200nm) were deposited in a circular transmission line model (CTLM) pattern. Prior to the fabrication of the patterns, the layers were degreased using acetone and ethanol in 5min steps and were rinsed with de-ionized (DI) water. Thereafter, they were boiled in aqua regia for 20min to remove the

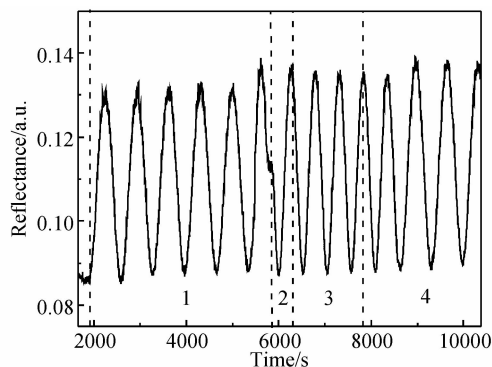


Fig. 2 In-situ reflectance measurement of the sample

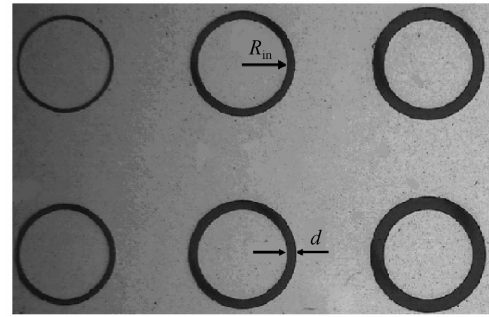


Fig. 3 Pattern of CTLM etching mask

native oxide. Figure 3 illustrates the actual etching mask imaged by microscopy. The CTLM ohmic pads were delineated using a lift-off process. The inner radius (R_{in}) of the pads is $120 \mu\text{m}$ and the gap spacing (d) between the inner and outer contact pads are 5, 10, 15, 20, 25, and $30 \mu\text{m}$, respectively.

The As-deposited samples were annealed at 450, 550, 600, 650, 670, 700, 750, and 850°C for 90s in an N_2 ambient using a rapid thermal annealing furnace (RTP-500). Then, the samples were annealed at 670°C for 30, 60, 90, 120, 300, and 600s, respectively. To extract the specific contact resistance using the CTLM, a current was supplied by one pair of probes, and another pair was used to measure the voltage between contacts. The X-ray diffractometer (XRD) analysis was carried out by D1-type high resolution X-ray diffractometer (HRXRD) measurements of Bede to study the contact formation mechanism.

3 Results and discussion

Current-voltage (I - V) measurements were made at room temperature using a Keithley 4200-SCS semiconductor characterization system. The I - V characteristics of the annealed ohmic contacts at different temperatures ($450, 550, 670, 750^\circ\text{C}$) for gap spacing of $15 \mu\text{m}$ are shown in Fig. 4. The ohmic contacts an-

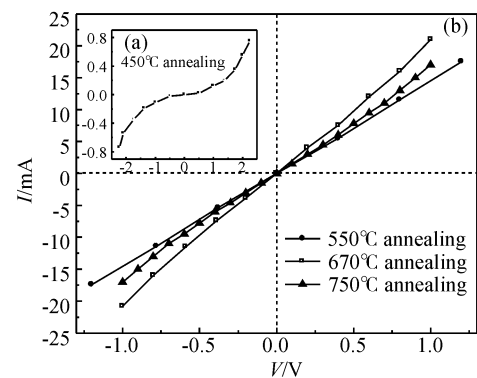
Fig. 4 (a) I - V curve of the annealed ohmic contact at 450°C for 90s; (b) I - V curves of the annealed ohmic contacts at 550, 670, and 750°C for 90s

Table 1 Specific contact resistivity ρ_c at different annealing temperatures

Annealing temperature / $^{\circ}\text{C}$	Annealing time /s	$\rho_c /(\Omega \cdot \text{cm}^2)$
550	90	1.21×10^{-3}
600	90	1.09×10^{-3}
650	90	5.75×10^{-4}
670	90	3.42×10^{-4}
700	90	7.34×10^{-4}
750	90	6.91×10^{-4}
850	90	9.40×10^{-4}

nealed over 550°C exhibit ohmic behaviour, while the 450°C annealing ohmic contact exhibits rectifying behaviour. This phenomenon indicates that the annealing temperature is an important factor for the mechanism of the ohmic contacts and that there is a limiting temperature in the formation of an ohmic contact. However, for different material and device structures, the temperature will be different. Chen *et al.*^[7] studied the contact of Ti/Al/Ni/Au to n-AlGaIn and they reported it was 400°C . In our experiment, the limiting temperature is about 550°C .

The values of the specific contact resistivity of the annealed ohmic contacts on pre-metallization treated surfaces are listed in Table 1. The CTLM results revealed that the contact resistance of the ohmic contacts decreased from 450 to 670°C , and thereafter increased as the annealing temperature increased to 850°C . The specific contact resistivity of the Ti/Al ohmic contact exhibited a minimum value of $3.42 \times 10^{-4} \Omega \cdot \text{cm}^2$ when the sample was annealed at 670°C for 90s.

In addition, we performed a comparison of different annealing times at 670°C . The annealing time was changed in the range of 30 to 600s, and included 30, 60, 90, 120, 300, and 600s. Figure 5 shows the specific contact resistivity ρ_c of the Ti/Al ohmic contacts. The minimum value of ρ_c was still $3.42 \times 10^{-4} \Omega \cdot \text{cm}^2$ when the sample was treated under 670°C an-

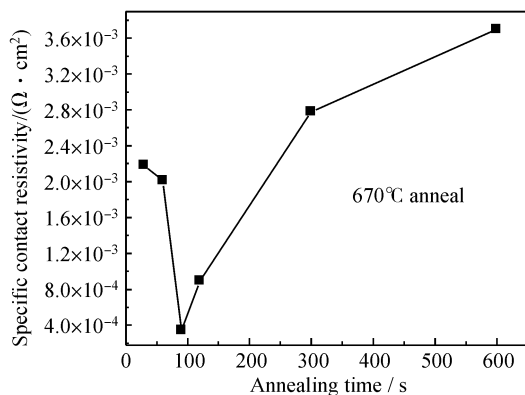
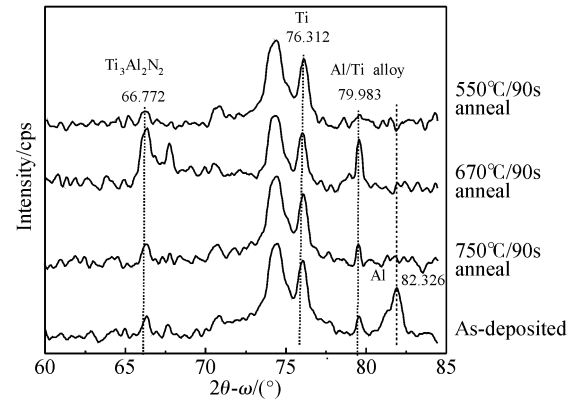
Fig. 5 Specific contact resistivity ρ_c for different annealing times

Fig. 6 XRD spectrums of the annealed ohmic contacts at different annealing temperatures

nealing for 90s. So, for this sample structure, the best annealing condition was about 670°C for 90s.

To characterize the chemical states of the samples, XRD examination was made of the Ti/Al contacts on n- $\text{Al}_{0.6}\text{Ga}_{0.4}\text{N}$ before and after annealing. Figure 6 shows the XRD spectra obtained from the metals/AlGaIn interface regions of the sample. The figure reveals that the peak of Ti lowered a certain amount after annealing and reached the lowest level at 670°C , and the peak of Al is barely observable. Meanwhile, a new phase peak-AlTi₃ at 79.983° was detected after annealing and reached its highest level at 670°C . This indicated that annealing caused Al atoms to diffuse through the Ti layer to form Al-Ti intermetallic phases with low work functions. These Al-Ti intermetallic phases can promote the formation of an ohmic contact in the AlGaIn surface^[6]. So, the higher the peak of Ti-Al alloy is, the better the ohmic contact that can be formed. This is in good agreement with the *I-V* results.

In addition, the peak of $\text{Ti}_3\text{Al}_2\text{N}_2$ was found to be 66.772° after 670°C annealing. The formation of $\text{Ti}_3\text{Al}_2\text{N}_2$ at the interface region indicates the outdiffusion of N atoms from the AlGaIn layer surface and hence the generation of N vacancies near the surface region of AlGaIn. These N vacancies are known to serve as donors in n-AlGaIn. Therefore, the annealing-induced improvement of the *I-V* characteristics of Ti/Al contacts could be attributed to the formation of $\text{Ti}_3\text{Al}_2\text{N}_2$ and as well as an Al-Ti intermetallic phase.

For solar-blind detectors, it is necessary to develop good ohmic contacts to improve the detectors' performances, such as small dark-current, large breakdown voltage, and high spectral responsivity. We fabricated back-illuminated solar-blind AlGaIn p-i-n detectors with the same structures but different ohmic contacts at 670°C annealing for 90s and with no annealing, respectively. Reverse bias *I-V* characteristics

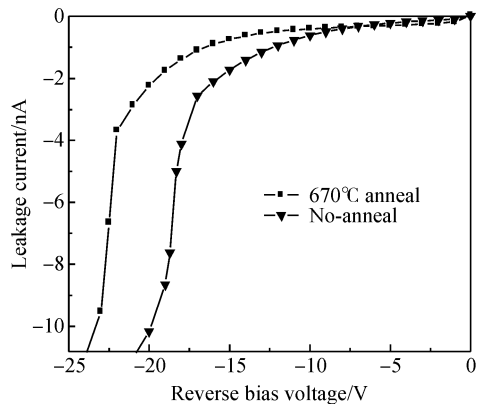


Fig.7 I - V curves of p-i-n detectors at reverse bias in the dark

of the p-i-n detectors in the dark are given in Fig. 7. The dark-current decreased after the 670°C annealing and its breakdown voltage improved.

In addition, spectral responsivity measurements of the two photodiodes were carried out in the 230~340nm spectral range at -1.5V reverse bias. Figure 8 shows the results of spectral responsivity measurements. The peak responsivities of the two samples all appeared at about 272nm. The annealed sample reached a maximum responsivity of 0.0764A/W at -1.5V bias and the non-annealed sample was only 0.0696A/W. Thus, the treatments on ohmic contacts

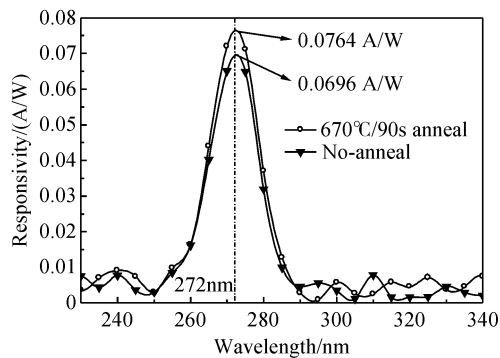


Fig. 8 Spectral responsivity versus wavelength curves at -1.5V bias for back-illuminated solar-blind AlGaIn p-i-n photodiode

can enhance the performances of the solar-blind p-i-n detectors.

4 Conclusion

To summarize, we have investigated the Ti/Al metallization scheme for the formation of ohmic contact on high-Al content $\text{Al}_{0.6}\text{Ga}_{0.4}\text{N}$ for solar-blind detectors. We show that the electrical properties of the Ti/Al contacts improved as the annealing temperature increased. In particular, the contact produced a very low specific contact resistivity, $3.42 \times 10^{-4} \Omega \cdot \text{cm}^2$, when annealed at 670°C for 90s. By X-ray diffraction measurement analysis, we found that the annealing-induced improvement of the I - V characteristics of Ti/Al contacts could be attributed to the formation of $\text{Ti}_3\text{Al}_2\text{N}_2$ and as well as an Al-Ti intermetallic phase. Using the ideal contact on back-illuminated solar-blind AlGaIn p-i-n detectors improved the spectral responsivity, dark-current, and breakdown voltage.

References

- [1] Adivarahan V, Simm G, Tamulaitis G, et al. Indium-silicon co-doping of high-aluminum-content AlGaIn for solar blind photodetectors. *Appl Phys Lett*, 2001, 79: 1903
- [2] Cao X A, Piao H, LeBoeuf S F, et al. Effects of plasma treatment on the ohmic characteristics of Ti/Al/Ti/Au contacts to n-AlGaIn. *Appl Phys Lett*, 2006, 89: 082109
- [3] Zhou H M, Shen B, Zhou Y G, et al. Metal/n-AlGaIn ohmic contact. *Chinese Journal of Semiconductors*, 2002, 23: 153 (in Chinese) [周慧梅, 沈波, 周玉刚, 等. 金属/n型 AlGaIn 欧姆接触. *半导体学报*, 2002, 23: 153]
- [4] Lin M E, Ma Z, Huang F Y, et al. Low resistance ohmic contacts on wide band-gap GaN. *Appl Phys Lett*, 1994, 64: 1003
- [5] Ruvimov S, Liliental-Weber Z, Washburn J, et al. Microstructure of Ti/Al and Ti/Al/Ni/Au ohmic contacts for n-GaN. *Appl Phys Lett*, 1996, 69: 1556
- [6] Luther B P, Mohny S E, Jackson T N, et al. Investigation of the mechanism for ohmic contact formation in Al and Ti/Al contacts to n-type GaN. *Appl Phys Lett*, 1997, 70: 57
- [7] Chen Jun, Li Xue, Li Xiangyang. Effect of rapid thermal annealing on Ti/Al/Ni/Au ohmic contact to n- $\text{Al}_{0.45}\text{Ga}_{0.55}\text{N}$. *International Workshop on Junction Technology*, 2006: 262

日盲探测器高 Al 组分 n- $\text{Al}_{0.6}\text{Ga}_{0.4}\text{N}$ 欧姆接触

朱雁翎^{1,†} 杜江锋¹ 罗木昌² 赵红² 赵文伯² 黄烈云² 姬洪¹ 于奇¹ 杨谟华¹

(1 电子科技大学电子薄膜与集成器件国家重点实验室, 成都 610054)

(2 重庆光电技术研究所, 重庆 400060)

摘要: 研究了应用于日盲探测器的高 Al 组分 Si 掺杂 n 型 $\text{Al}_{0.6}\text{Ga}_{0.4}\text{N}$ 与两层金属层 Ti(20nm)/Al(100nm) 之间的欧姆接触. 在制作金属电极前用煮沸王水对样片进行表面预处理, 金属制作后再在 N_2 氛围中做快速热退火处理. 使用高精度 XRD 测试样品表面特性, 并对不同温度下的情况进行比较. 样品的比接触电阻率是用环形传输线模型通过 $I-V$ 测试得到. 670°C 下 90s 退火得到最优 ρ_c 为 $3.42 \times 10^{-4} \Omega \cdot \text{cm}^2$. 将该处理方法应用到实际的背照式 AlGaIn p-i-n 日盲探测器中, 探测器的光谱响应度和反向特性等参数得到很大的优化.

关键词: 高铝 n-AlGaIn; 欧姆接触; 退火; 背光照; pin 日盲探测器

PACC: 2940P; 6150C **EEACC:** 4250

中图分类号: O47 **文献标识码:** A **文章编号:** 0253-4177(2008)09-1661-05

† 通信作者. Email: yanlz83@163.com

2008-03-26 收到, 2008-05-07 定稿